

SANDIA REPORT

SAND2017-11054

Unlimited Release

Printed October 2017

Thermal Decomposition Model Development of EN-7 and EN-8 Polyurethane Elastomers

Ryan Keedy, Kale Harrison, and Joseph Cordaro

Prepared by
Sandia National Laboratories
Albuquerque, New Mexico 87185 and Livermore, California 94550

Sandia National Laboratories is a multimission laboratory managed and operated by National Technology and Engineering Solutions of Sandia LLC, a wholly owned subsidiary of Honeywell International Inc. for the U.S. Department of Energy's National Nuclear Security Administration under contract DE-NA0003525.

Approved for public release; further dissemination unlimited.



Sandia National Laboratories

Issued by Sandia National Laboratories, operated for the United States Department of Energy by Sandia Corporation.

NOTICE: This report was prepared as an account of work sponsored by an agency of the United States Government. Neither the United States Government, nor any agency thereof, nor any of their employees, nor any of their contractors, subcontractors, or their employees, make any warranty, express or implied, or assume any legal liability or responsibility for the accuracy, completeness, or usefulness of any information, apparatus, product, or process disclosed, or represent that its use would not infringe privately owned rights. Reference herein to any specific commercial product, process, or service by trade name, trademark, manufacturer, or otherwise, does not necessarily constitute or imply its endorsement, recommendation, or favoring by the United States Government, any agency thereof, or any of their contractors or subcontractors. The views and opinions expressed herein do not necessarily state or reflect those of the United States Government, any agency thereof, or any of their contractors.

Printed in the United States of America. This report has been reproduced directly from the best available copy.

Available to DOE and DOE contractors from

U.S. Department of Energy
Office of Scientific and Technical Information
P.O. Box 62
Oak Ridge, TN 37831

Telephone: (865) 576-8401
Facsimile: (865) 576-5728
E-Mail: reports@osti.gov
Online ordering: <http://www.osti.gov/scitech>

Available to the public from

U.S. Department of Commerce
National Technical Information Service
5301 Shawnee Rd
Alexandria, VA 22312

Telephone: (800) 553-6847
Facsimile: (703) 605-6900
E-Mail: orders@ntis.gov
Online order: <http://www.ntis.gov/search>



Thermal Decomposition Model Development of EN-7 and EN-8 Polyurethane Elastomers

Ryan Keedy¹, Kale Harrison², Joseph Cordaro³

¹ Thermal/Fluid Science Engineering

² Security Systems

³ Materials Chemistry

Sandia National Laboratories

P.O. Box 5800

Livermore, California 94550

Abstract

Thermogravimetric analysis – gas chromatography/mass spectrometry (TGA-GC/MS) experiments were performed on EN-7 and EN-8, analyzed, and reported in [1]. This SAND report derives and describes pyrolytic thermal decomposition models for use in predicting the responses of EN-7 and EN-8 in an abnormal thermal environment.

CONTENTS

2.	Decomposition Kinetics	8
2.1.	EN-7	10
2.2.	EN-8	13
3.	Isothermal Experiment Comparison	15
4.	Decomposition Products	17
5.	Discussion	21
6.	References	22

FIGURES

Figure 1: Experimental TGA data of EN-7 (top) and EN-8 (bottom) at four different heating rates; on the left is the mass loss and on the right is the corresponding temperature derivative	8
Figure 2: Derivative of each of the optimized reactions in addition to the experimental TGA data for EN-7 subject to a 10 °C/min heating rate	11
Figure 3: Experimental TGA data and model predictions of EN-7 decomposition at four different heating rates; on the left is the derivative of mass loss with respect to temperature, and on the right is the corresponding mass loss as a percentage of the original mass	12
Figure 4: Experimental TGA data and model predictions of EN-8 decomposition at four different heating rates; on the left is the derivative of mass loss with respect to temperature, and on the right is the corresponding mass loss as a percentage of the original mass	14
Figure 5: Results of isothermal decomposition at three different temperatures from both TGA experiments [1] (left) and simulation using the derived model kinetics (right)	15
Figure 6: Comparison of the time derivative of mass loss at from experiment and simulation for 5 °C/min heating rate at low temperatures	16
Figure 7: Capture time intervals for EN-7 and EN-8 GC/MS analysis, from [1].....	17
Figure 8: MS data for peaks produced by GC experiments.....	17
Figure 9: Partial structure of EN-7/8 detailing two urethane linkages [RNHCOOR], where R represents the rest of the molecule.....	19
Figure 10: Comparison of thermal decomposition predictions for four heating rates for both EN-7 and EN-8	21

TABLES

Table 1: Preliminary description of foam decomposition reactions	9
Table 2: Kinetic parameters for thermal decomposition of EN-7	10
Table 3: Kinetic parameters for thermal decomposition of EN-8	13
Table 4: List of decomposition products based on MS results from Figure 8.....	18
Table 5: Description of foam decomposition reactions	21

1. INTRODUCTION

Thermogravimetric analysis – gas chromatography/mass spectrometry (TGA-GC/MS) experiments were performed on the polyurethane elastomers EN-7 and EN-8, analyzed, and reported in [1]. By characterizing the decomposition process and products, Sandia National Laboratories can gain a more complete picture about how these materials will behave under abnormal environments. Furthermore, this work bridges a gap uncovered during thermal modeling and simulation performed by Silva et al. as part of the W78 program. This SAND report derives and describes thermal decomposition models for use in predicting the responses of EN-7 and EN-8 in an abnormal thermal environment.

2. DECOMPOSITION KINETICS

TGA-GC/MS experiments were performed in both unconfined and partially confined configurations. The difference is that in the partially confined configuration, the crucible (5 mm diameter) containing the foam sample is covered with a lid with a small pinhole in it (approximately 1 mm diameter); the unconfined case has no cover.

In this analysis, the focus will be on development of models associated with the partially confined case. This configuration has been chosen for other model development due to the potential build-up of back pressure through the pinhole orifice. It is expected that thermal decomposition in abnormal environments occurs subject to some degree of back pressure.

TGA-GC/MS decomposition experiments were conducted on both EN-7 and EN-8 at various heating rates: 5, 10, 15, and 20 °C/min. The mass loss associated with the experiments, as well as the derivative with respect to temperature are plotted in Figure 1. It is important to consider several heating rates since the decomposition is time dependent, and not simply a function of temperature.

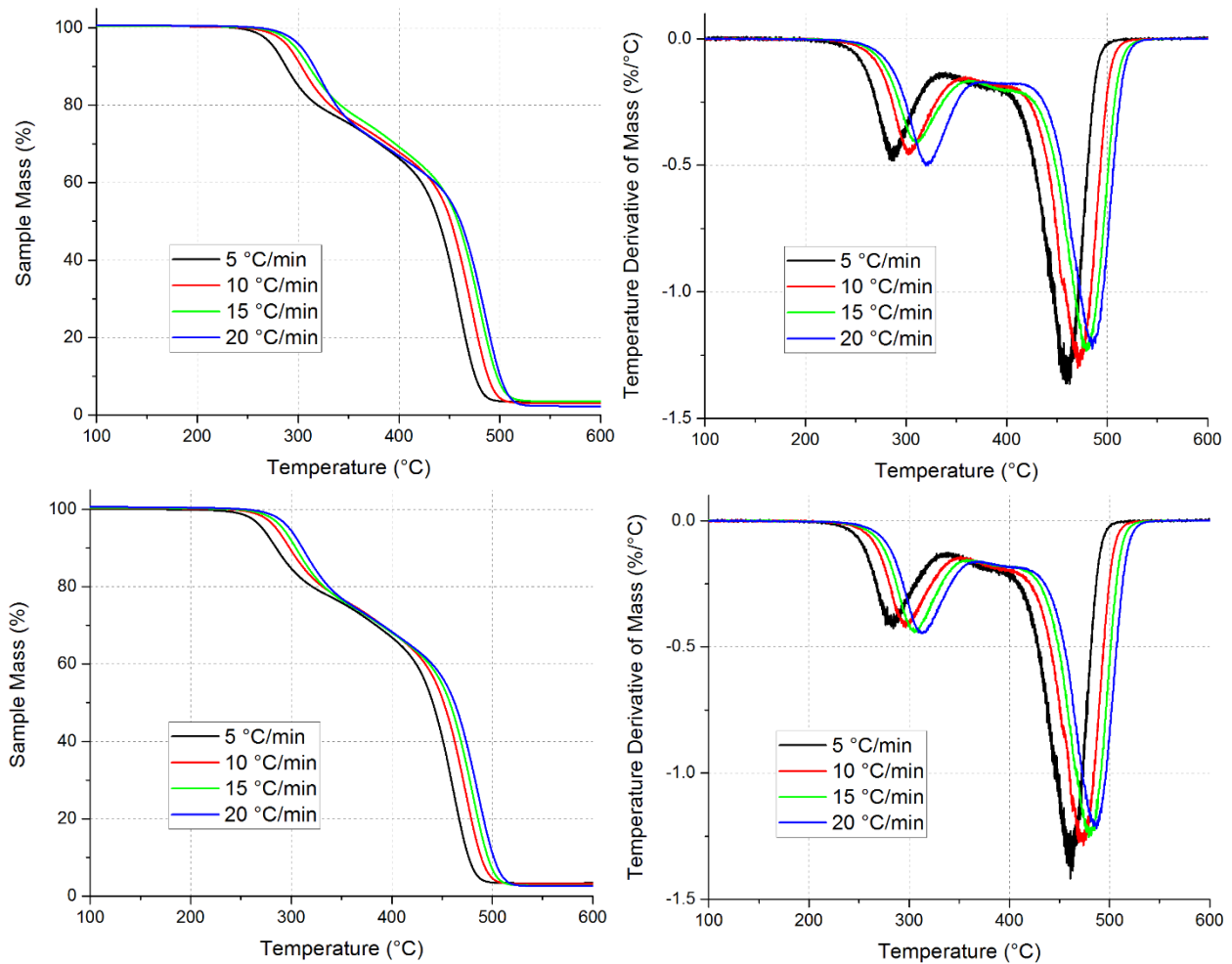


Figure 1: Experimental TGA data of EN-7 (top) and EN-8 (bottom) at four different heating rates; on the left is the mass loss and on the right is the corresponding temperature

derivative

The model developed for the decomposition should recreate all of the curves from Figure 1. This creates a large number of constraints, and since the model is only an approximation to the physics of the problem, it will involve compromises in the quality and flexibility of the fit across all heating rates. In order to create the most appropriate model for computational analyses, the heating rates for fitting were limited to 5-20 °C/min (higher heating rates are considered unlikely to be experienced in real-world scenarios).

Based on the derivative of the decomposition in Figure 1 and literature describing polyurethane decomposition [2], it is assumed that for both EN-7 and EN-8, the decomposition process consists of three distinct, independent reactions, whose peaks are located at approximately 300, 375, and 475 °C.

Let the polymer matrix consist of moieties B_i that decompose by different mechanisms to form species D_{ij} (designating the j^{th} species produced by decomposition of moiety B_i). Let w_i^0 denote the mass fraction of B_i in the initial foam, and let ξ_{ij} denote the mass fraction of B_i that forms D_{ij} . Decomposition products D_{ij} can be light gases, organic compounds, and thermally stable condensed-phase products (char). Table 1 details the description of the model for the three reactions involved in the decomposition (see the section **Decomposition Products** for a detailed discussion of the number and type of decomposition products associated with each reaction).

Table 1: Preliminary description of foam decomposition reactions

Initial Foam ($w_1^0 B_1 + w_2^0 B_2 + w_3^0 B_3$)	Reaction i \rightarrow	Decomposition Products
B_1	$\frac{dB_1}{dt}$	$\xi_{11} D_{11} + \xi_{12} D_{12}$
B_2	$\frac{dB_2}{dt}$	$\xi_{21} D_{21}$
B_3	$\frac{dB_3}{dt}$	$\xi_{31} D_{31} + \xi_{32} D_{32}$

The reaction rate associated with reaction i is defined as:

$$\frac{d[B_i]}{dt} = k_i(T)[B_i]^{n_i}$$

where $[B_i]$ is the normalized component i of the foam subject to decomposition, and n_i defines the order of reaction i . Furthermore, $k_i(T)$ is the rate constant associated with the decomposition of reaction i , and takes the form of the Arrhenius equation:

$$k_i(T) = A_i e^{-E_i/RT}$$

where A_i is the pre-exponential factor, E_i is the activation energy, R is the gas constant, and T is the temperature.

To determine the most appropriate values for the kinetic coefficients associated with each reaction, Dakota [2] was used for optimization. The objective function consists of the difference between experiment and model of the temperature derivative of the mass loss for all four heating rates. The optimization procedure is more thoroughly described in [3] (see [4] for application example). The four parameters to be optimized are as follows:

- E_i/R : The ratio of the activation energy (E_i) to the gas constant (R)
- $\ln A_i$: The natural log of the pre-exponential factor (A_i)
- n_i : The order of the reaction
- w_i^0 : The mass fraction of the virgin foam associated with the reaction

2.1. EN-7

Table 2 contains the optimized parameters associated with each of the four parameters for each of the three reactions for EN-7.

Table 2: Kinetic parameters for thermal decomposition of EN-7

	Activation Energy, E_i (kJ/mol)	ln Pre-Exponential Factor ($1/sec^{n_i}$)	Order, n_i	Mass Fraction, w_i^0
Reaction 1	175	36.0	2.00	0.247
Reaction 2	230	41.7	2.24	0.106
Reaction 3	239	37.7	1.00	0.623 [0.647]

When each reaction is plotted separately (as seen in Figure 2), it is clear how each contributes to the overall mass loss derivative. Furthermore, the reactions correspond to the peaks identified in Figure 1.

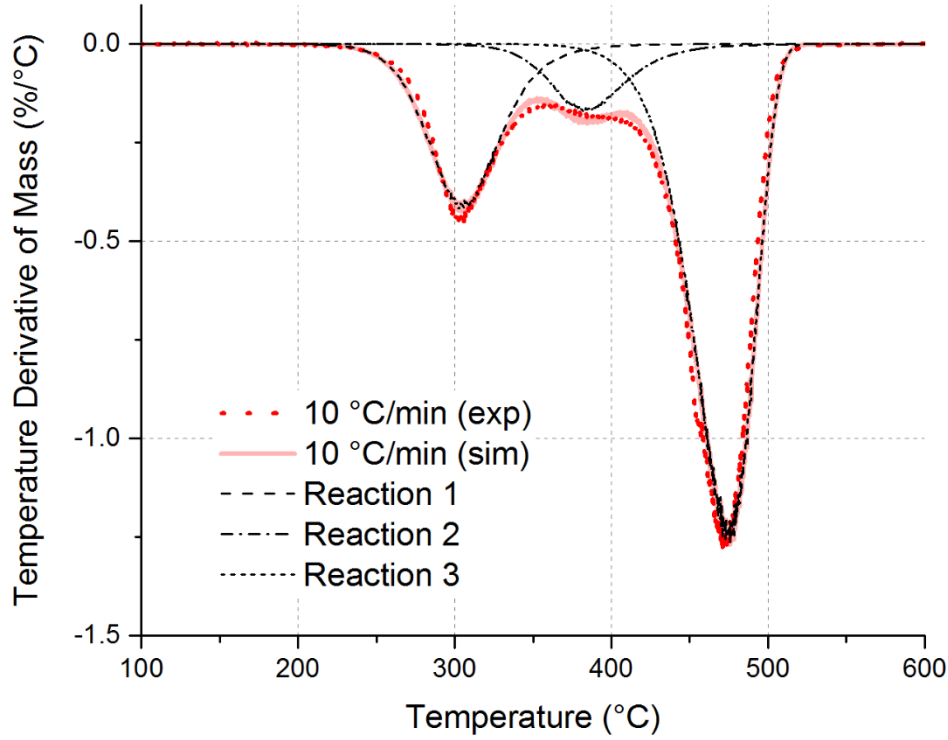
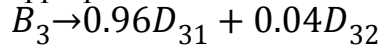


Figure 2: Derivative of each of the optimized reactions in addition to the experimental TGA data for EN-7 subject to a 10 °C/min heating rate

The mass fractions sum to 0.976, leaving 0.024 uninvolved in the decomposition (meaning the decomposition curve will asymptote to 0.024). Knowing that the remaining mass is not unreacted foam, but instead, a solid product of decomposition (char), this must be accounted for in the reactions. Without more detailed knowledge about the nature of the reactions, it is difficult to attribute the solid decomposition product (char) to any single reaction. For simplicity, it is assumed here that the third reaction, accounting for the largest proportion of foam, will decompose into char (as well as gas). This requires adjusting the mass fraction, w_3^0 , to 0.647. In order to get the correct proportion of products, the reaction can be rewritten with appropriate substitutions for ξ_{3j} :



where D_{31} is associated with the gas products, and D_{32} is associated with char products. Figure 2 has shown excellent agreement for 10 °C/min; Figure 3 confirms the model works across all of the heating rates under consideration, as the model curves also shift to higher temperatures for faster heating rates.

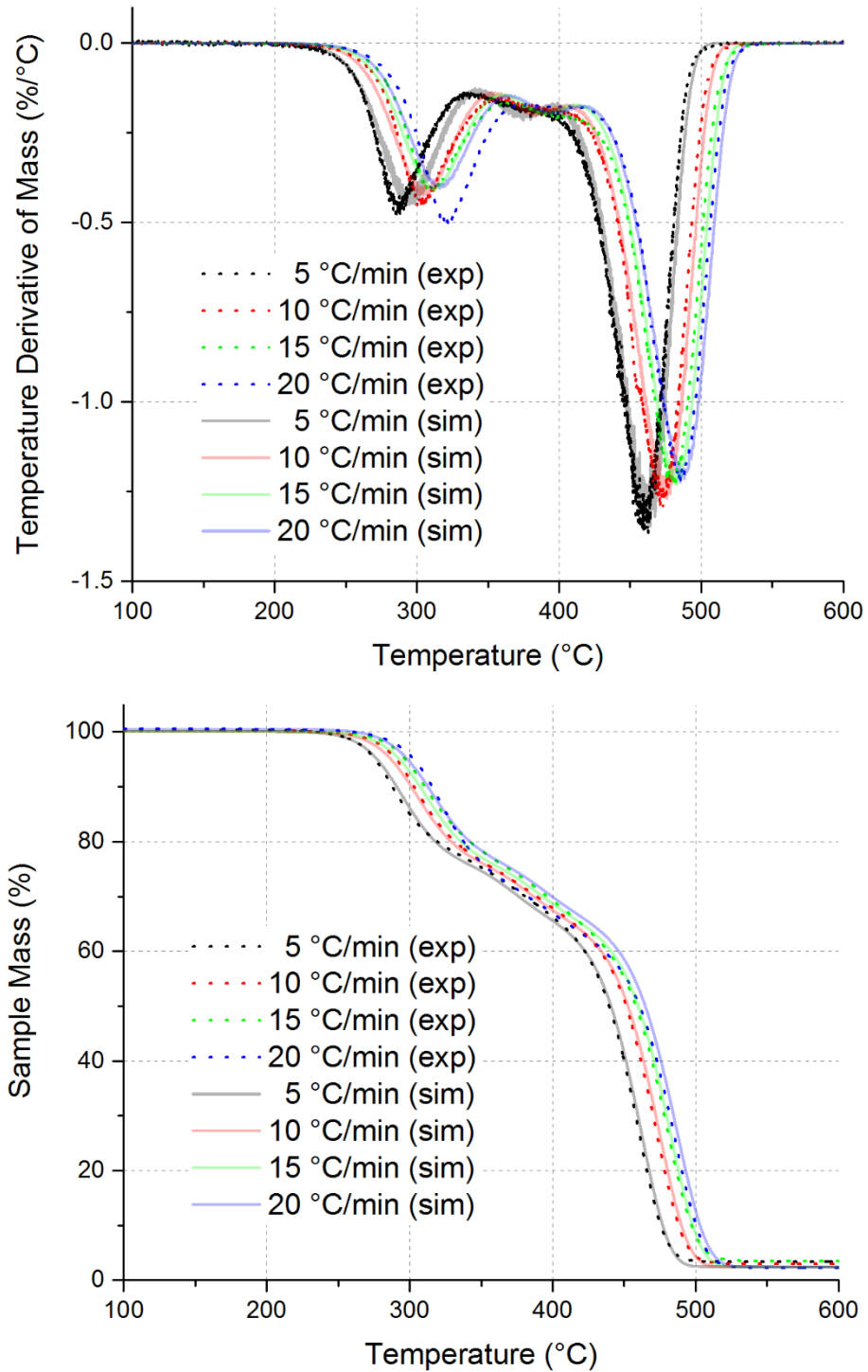


Figure 3: Experimental TGA data and model predictions of EN-7 decomposition at four different heating rates; on the top is the derivative of mass loss with respect to temperature, and on the bottom is the corresponding mass loss as a percentage of the original mass

2.2. EN-8

As is the case for the EN-7, partially confined TGA-GC/MS experiments were performed on EN-8 at several heating rates. Figure 1 shows experimental results of mass loss and the derivative of mass loss with respect to temperature for heating rates of 5, 10, 15, and 20 °C/min.

Due to the similarities between EN-7 and EN-8 displayed in Figure 1, optimization proceeded with the same assumptions (three reactions, identical initial conditions). The results of the optimization for the twelve parameters of interest are presented in Table 3.

Table 3: Kinetic parameters for thermal decomposition of EN-8

	Activation Energy, E_i (kJ/mol)	ln Pre-Exponential Factor ($1/sec^{n_i}$)	Order, n_i	Mass Fraction, w_i^0
Reaction 1	175	36.2	2.23	0.246
Reaction 2	231	41.7	2.20	0.102
Reaction 3	238	37.6	1.00	0.627 [0.652]

The same steps to account for char are taken as is the case with EN-7. The mass fraction, w_3^0 , is adjusted to 0.652 such that the sum of all mass fractions is unity. The coefficients associated with the decomposition products are assumed to remain the same as EN-7: $\xi_{31} = 0.96$ and $\xi_{32} = 0.04$.

Figure 4 shows the quality of the agreement between the simulations and experiments across all four heating rates.

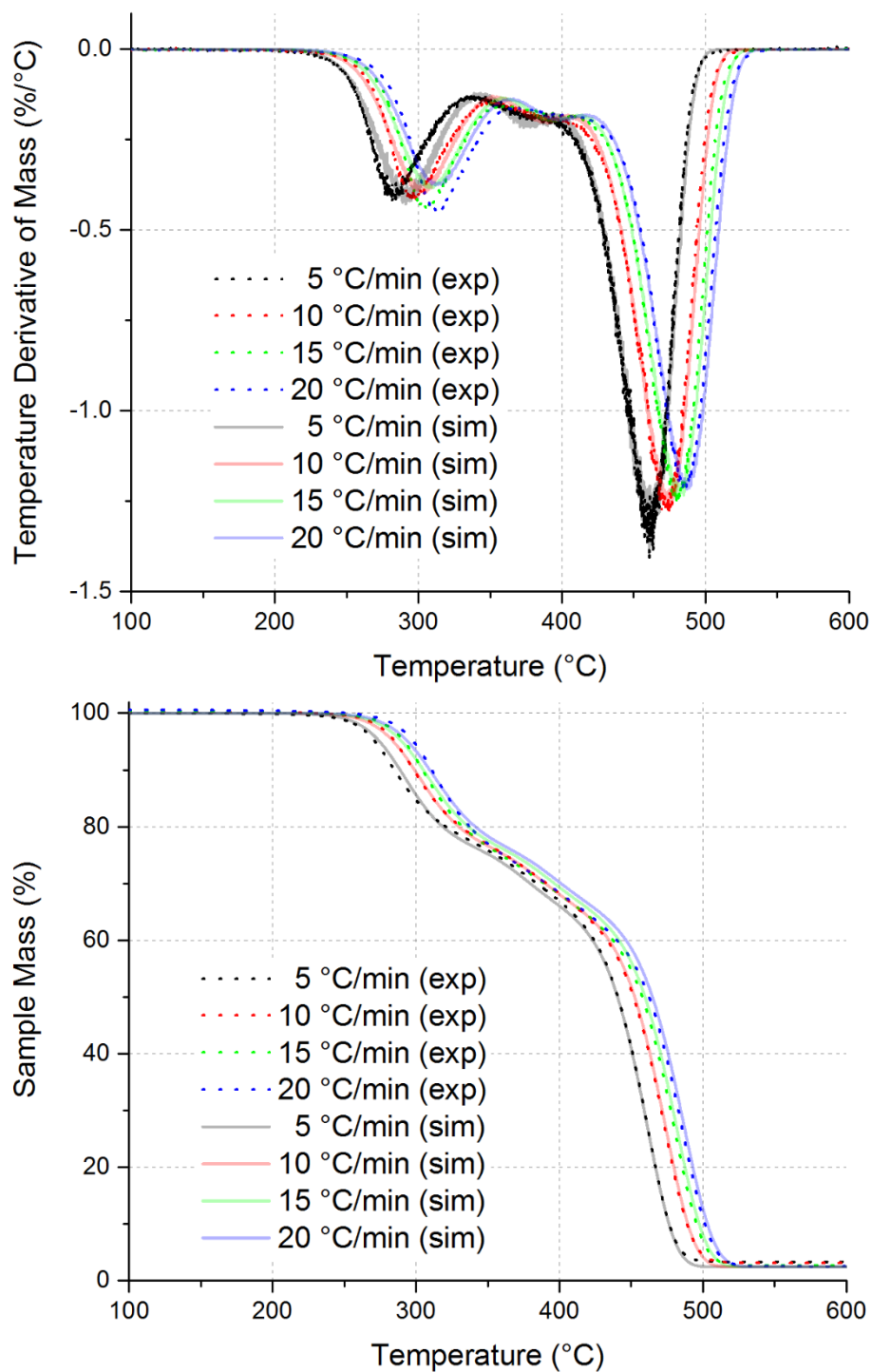


Figure 4: Experimental TGA data and model predictions of EN-8 decomposition at four different heating rates; on the top is the derivative of mass loss with respect to temperature, and on the bottom is the corresponding mass loss as a percentage of the original mass

3. ISOTHERMAL EXPERIMENT COMPARISON

In addition to the TGA experiments that were conducted at different heating rates, [1] also reported on mass loss as a function of time for several isothermal tests. Figure 5 shows the results from both the experiments and simulations of the same conditions. While the trends are quite similar, the magnitudes of the differences in response between experiments and simulations are quite different, especially at the lower temperatures.

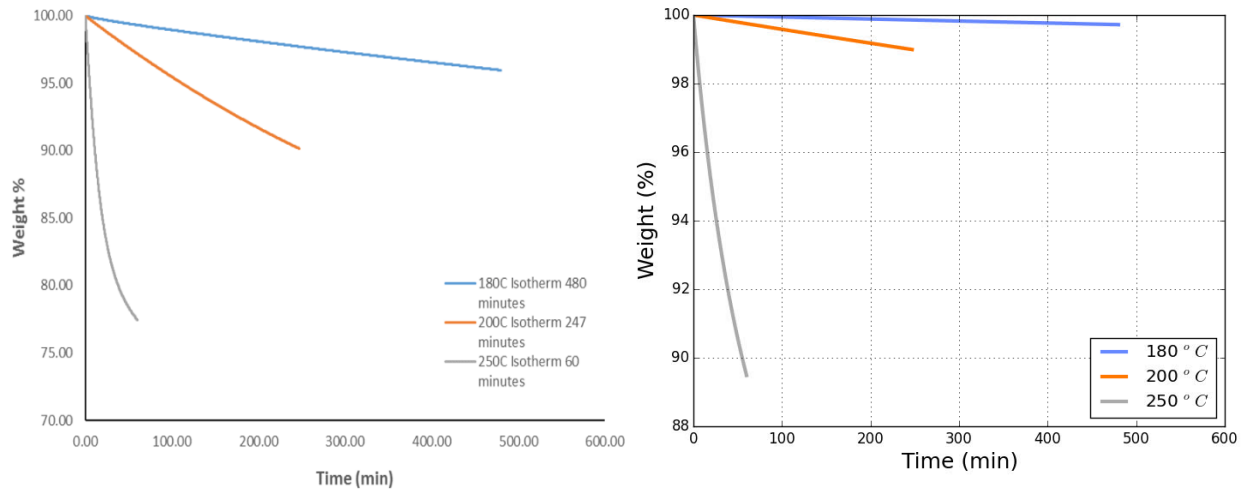


Figure 5: Results of isothermal decomposition at three different temperatures from both TGA experiments [1] (left) and simulations using the derived model kinetics (right)

The results from Figure 5 can be explained by examining the difference in the decomposition rates at the different temperatures. Figure 6 shows the time derivative of both the experiment and simulation at 5 °C/min. Across the range of 180 °C to 250 °C, the experimental mass loss rate is more pronounced than the model prediction. At very low temperatures (e.g. 180 °C to 200 °C), the model predictions are so close to zero that even small magnitude differences in the rate loss correspond to large ratios, that when integrated over a long period of time (as is the case for isothermal experiments), will lead to large discrepancies. Fortunately, many of the abnormal thermal applications for this model do not coincide with this type of heating regime.

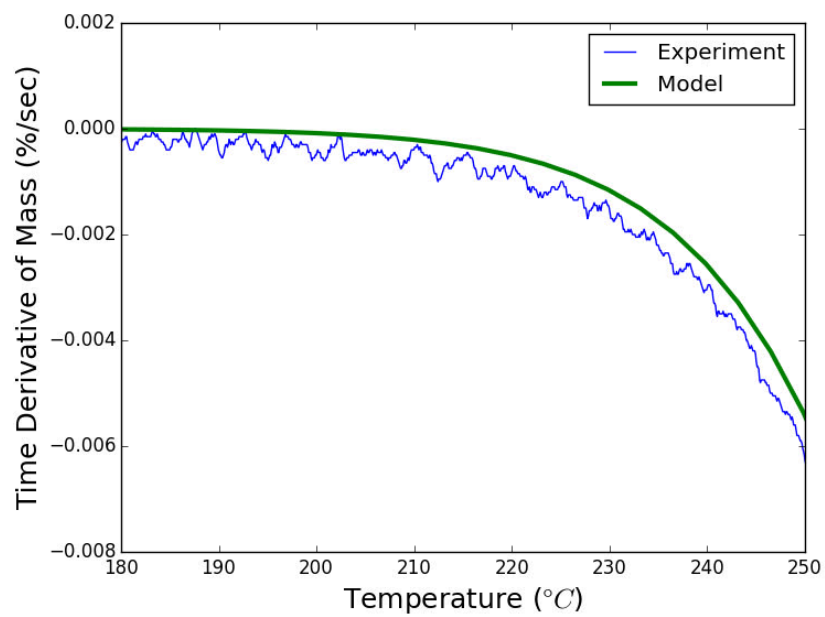


Figure 6: Comparison of the time derivative of mass loss at from experiment and simulation for 5 °C/min heating rate at low temperatures

4. DECOMPOSITION PRODUCTS

In addition to unconfined TGA data, GC/MS data were also collected for 10 °C/min heating rates [1]. The data were collected by sampling the TGA products over the entire decomposition range (see Figure 7 for detailed accounting of the collection times). Due to the consistency between EN-7 and EN-8 measurements, the following analysis will apply to both foams.

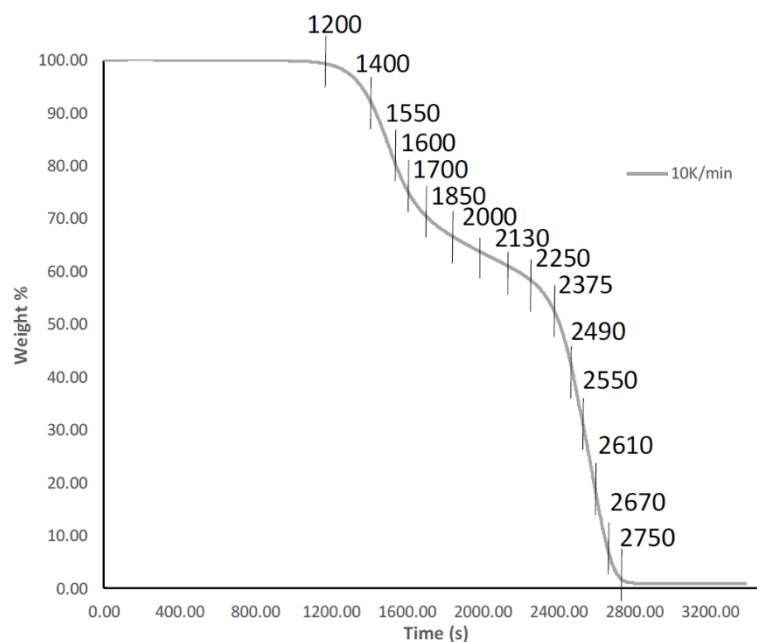


Figure 7: Capture time intervals for EN-7 and EN-8 GC/MS analysis, from [1]

At each collection time indicated, gaseous products are separated according to the residence time in the GC column. The gas is then ionized and sent to the mass spectrometer, where ions are detected on the basis of their mass to charge ratio. The data are displayed as a total ion chromatogram. Further information is obtained by analyzing the peaks in the total ion chromatogram, since each peak represents a detected compound and contains the mass to charge ratio information that can be used to identify that compound (see Figure 8 for examples of MS data). Comparison of these data to a spectral library suggests candidates for the molecules associated with the two GC peaks of interest (see Table 4).

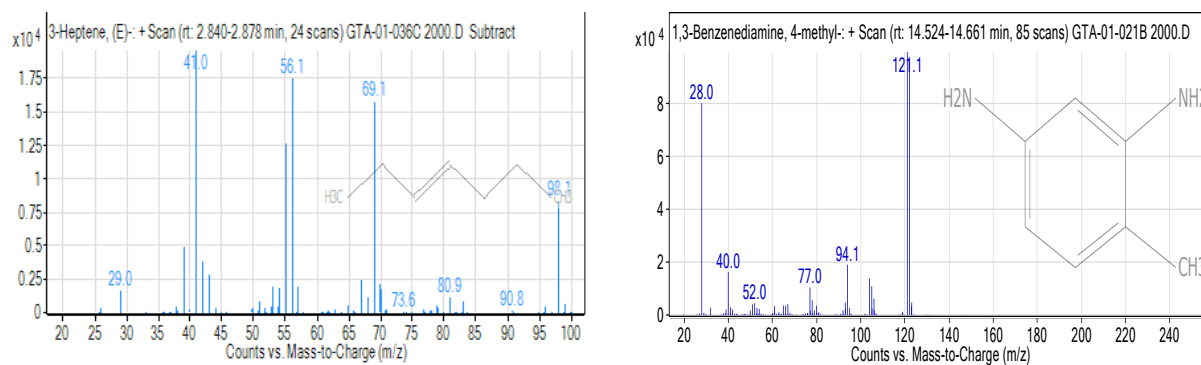
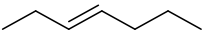
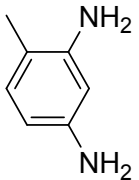


Figure 8: MS data for peaks produced by GC experiments

Table 4: List of decomposition products based on MS results from Figure 8

Retention Time (min)	Likely Molecule			
	Name	Chemical formula	Molecular weight (g/mol)	Representation
1.3	Nitrogen, Carbon dioxide	N_2 , CO_2	28, 44	$N \equiv N$ and $O = C = O$
2.9	3-Heptene	C_7H_{14}	98	
14.6	Diaminotoluene	$C_7H_{10}N_2$	122	

Two peaks recurred throughout MS data: 28 (m/z) and 44 (m/z). Since nitrogen is used as a carrier gas for the TGA, it is clear that 28 (m/z) is associated with N_2 . It is very likely that CO_2 represents a portion of the collected gas, due to both the presence of the 44 (m/z) peak and knowledge about the mechanisms for EN decomposition.

It is not realistic to presume that Table 4 is a comprehensive list of the decomposition products, but in order to create a straightforward engineering model, the decomposition products in the model will focus on those products.

Assume that the basis molecule for the decomposition mechanism is described by the diagram in Figure 9 (from [1]). The decomposition evolution of the urethane linkages is undoubtedly quite complex; it is likely that products will themselves decompose, or react with other products in a series of reactions that could be contingent on previous reactions. However, recall that the simplifying assumption of this model is to assume that both EN-7 and EN-8 consist of three moieties (B_1 , B_2 , B_3) which each have independent decomposition reactions described in Table 1. The discussion of the chemistry that follows serves as a guide for defining the parameters associated with the engineering model.

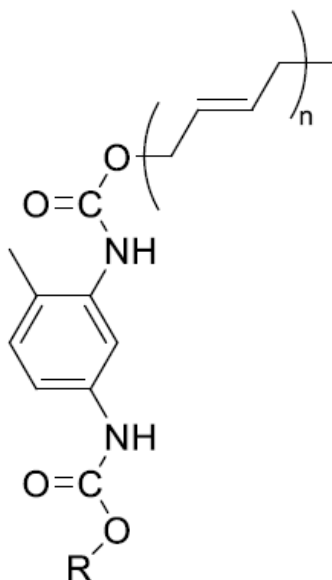
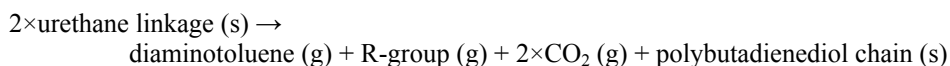


Figure 9: Partial structure of EN-7/8 detailing two urethane linkages [RNHCOOR], where R represents the rest of the molecule

Referring to Figure 2, the reaction which peaks at approximately 300 °C is associated with the first mechanism of decomposition in which it is assumed that urethane linkages will decompose into four main constituents:

- Diaminotoluene (gas) – associated with 14.6 min (Table 4)
- R-group (gas) – associated with 2.9 min (Table 4)
- CO₂ (gas) – associated with 1.3 min (Table 4)
- Polybutadienediol chain (solid)



The decomposition reaction associated with the first reaction is associated with two different reaction products; D_{11} is associated with CO₂ (44 g/mol), and D_{12} is associated with the higher molecular weight decomposition products (diaminotoluene and R-group). Based on the results of the GC/MS, it appears R-groups may gasify as heptene (98 g/mol) or similar. Because of the uncertainty of the gasification of the R-groups, an average molecular weight of 122 g/mol will be selected in order to be consistent with diaminotoluene. In order to get the correct proportion of products, the reaction can be rewritten with appropriate substitutions for ξ_{1j} . A single mole of B_1 will produce two moles each of D_{11} (CO₂) and D_{12} (high molecular weight gases). The resulting mass ratios will lead to the following distribution by mass:

$$B_1 \rightarrow 0.265D_{11} + 0.735D_{12}$$

The second and third peaks of decomposition (see Figure 2) are presumed to be associated with the decomposition and gasification of the polybutadiene. In fact, the decomposition peaks are

consistent with the description of thermal degradation of polybutadiene in [5]. The higher temperatures result in a number of different decomposition products, such as linear alkenes, linear alkanes, and cycloalkenes. The work of [5] details ethane, propane, propene, butadiene, butane, 4-vinylcyclohexene and others. Lacking a conclusive distribution of decomposition products, the assumption will be made that the second and third peaks will yield gases with an average molecular weight of 50 g/mol. A liberal uncertainty should be applied to this molecular weight to reflect the lack of detailed knowledge.

5. DISCUSSION

Note that the parameters described in Table 2 and Table 3 are nearly identical for both EN-7 and EN-8. The largest difference is the order of the first reaction (2.00 versus 2.23). This is consistent with the graph of TGA experiments for multiple heating rates for both foams in Figure 10. It appears that for a given heating rate, the both EN-7 and EN-8 decompose very similarly, especially at high temperatures. Given their nearly identical formulations, this consistency in decomposition is unsurprising.

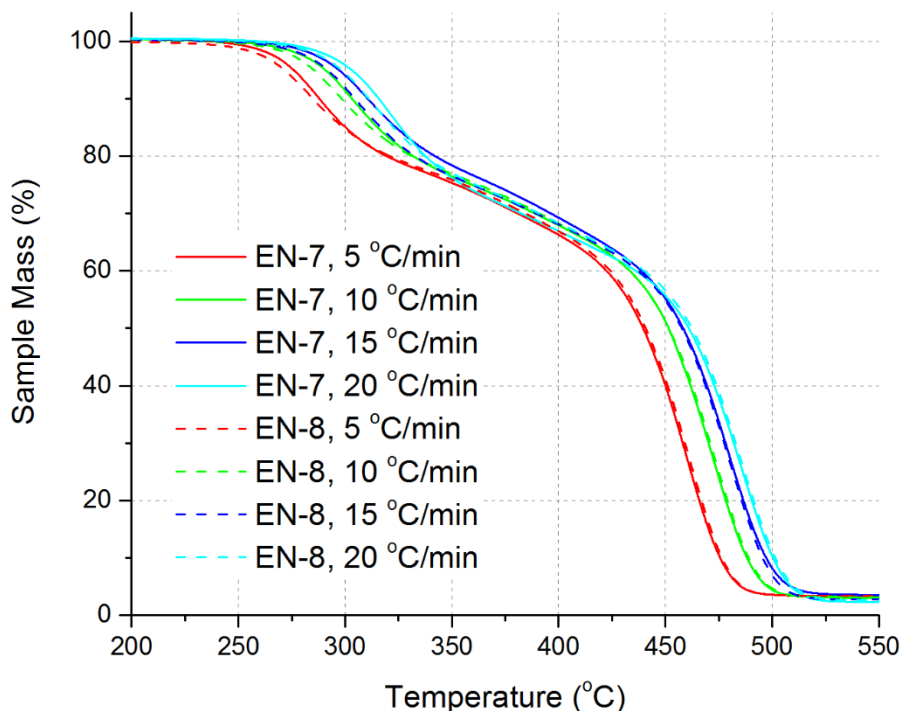


Figure 10: Comparison of thermal decomposition predictions for four heating rates for both EN-7 and EN-8

Having detailed the specifics of the three different reactions within the engineering model, it is useful to reconstruct Table 1 as Table 5 below. The table is representative for both EN-7 and EN-8 models.

Table 5: Description of foam decomposition reactions

Initial Foam $(w_1^0 B_1 + w_2^0 B_2 + w_3^0 B_3)$	Reaction i \rightarrow	Decomposition Products
B_1	$\frac{dB_1}{dt}$	$0.265D_{11} + 0.735D_{12}$
B_2	$\frac{dB_2}{dt}$	D_{21}
B_3	$\frac{dB_3}{dt}$	$0.96D_{31} + 0.04D_{32}$

6. CONCLUSIONS

Thermal decomposition models have been developed for both EN-7 and EN-8. The models are based on data taken at heating rates from 5 to 20 °C/min from pyrolytic TGA experiments [1]. For both EN-7 and EN-8, three independent Arrhenius decomposition reactions were fit to the experimental data according to a least-squares fit.

As demonstrated by Figure 1 and Figure 10, the decomposition curves for EN-7 and EN-8 are very similar. As such, the models for them share many characteristics. The fitted Arrhenius coefficients and initial mass distribution (see Table 2 and Table 3) as optimized by Dakota are consistent between EN-7 and EN-8. Their decomposition products, as indicated by GC/MS experiments, are defined to be identical (see Table 5).

7. REFERENCES

- [1] K. Harrison, D. Murtagh and J. Cordaro, "Thermal Degradation Investigation of Polyurethane Elastomers using Thermal Gravimetric Analysis – Gas Chromatography/Mass Spectrometry," Sandia National Laboratories, Livermore, CA, 2016.
- [2] D. Allan, J. Daly and J. Liggat, "Thermal volatilisation analysis of TDI-based flexible polyurethane foam," *Polymer Degradation and Stability*, vol. 98, no. 2, pp. 535-541, 2013.
- [3] B. Adams, L. Bauman, W. Bohnhoff, K. Dalbey, M. Ebeida, J. Eddy, M. Eldred, P. Hough, K. Hu, J. Jakeman, L. Swiler and D. Vigil, "DAKOTA, A Multilevel Parallel Object-Oriented Framework for Design Optimization, Parameter Estimation, Uncertainty Quantification, and Sensitivity Analysis: Version 5.4 User's Manual," Sandia National Laboratories, Albuquerque, NM, 2013.
- [4] R. Keedy, "Parameter Estimation Procedure for Organic Material Decomposition," Sandia National Laboratories, Livermore, CA, 2016.
- [5] R. Keedy, "Ablefoam Thermal Decomposition Model Development," Sandia National Laboratories, Livermore, CA, 2017.
- [6] M. P. Luda, M. Guaita and O. Chiantore, "Thermal degradation of polybutadiene, 2. Overall thermal behaviour of polymers with different microstructures," *Macromolecular Chemistry and Physics*, vol. 193, no. 1, pp. 113-121, 1992.

DISTRIBUTION

1	MS0483	Linda Jones	2223
1	MS0483	Derek Wartman	2223
1	MS0825	Roy Hogan	1514
1	MS0828	Benjamin Schroeder	1544
1	MS0828	Humberto Silva	1514
1	MS0840	Kyle Smith	1533
1	MS1135	Kathryn Hoffmeister	1532
1	MS1135	James Nakos	1532
1	MS1135	Ethan Zepper	1532
1	MS9110	Paul Yoon	8220
1	MS9957	Victor Brunini	8253
1	MS9957	Tricia Gharagozloo	8253
1	MS9957	Sarah Scott	8253
1	MS0899	Technical Library	9536 (electronic copy)

